Output Impedance Modeling of a Multilevel Modular Switched-Capacitor Converter to Achieve Continuously Variable Conversion Ratio

Mohammed Khorshed Alam and Faisal H. Khan

Power Engineering and Automation Research Lab (PEARL)
Dept. of Electrical and Computer Engineering,
University of Utah, Salt Lake City, Utah, USA
Email: khorshed.alam@utah.edu

Abstract— **The multilevel modular capacitor clamped dc-to-dc converter (MMCCC) topology is completely modular and belongs to two-phase switched capacitor converter group. The conversion ratio of an ideal MMCCC converter in step-up mode is an integer and depends on the number of modules used. For a *k*-module MMCCC, the maximum up-conversion ratio is (*k*+1), and it has already been shown in literature that different integer conversion ratios can be achieved by changing the active number of modules of an MMCCC. In this paper, different methods are proposed for MMCCC in order to achieve fractional conversion ratios (CR) in step-up mode without changing the complementary two-phase switching orientation. Fractional CRs can be obtained in several switched-capacitor circuits at the cost of significantly lower efficiency. However, MMCCC with the aid of a new pulse dropping technique can produce fractional CR while maintaining high efficiency. The variation in efficiency and equivalent resistance as a function of frequency has been analyzed in this paper. Simulation and experimental results using a reconfigurable 5-module MMCCC prototype have been used to validate the new control scheme.**

I. INTRODUCTION

Switched capacitor (SC) converters have many advantageous features compared to inductor based dc-dc converters. As there are no magnetic components used, SC converters can be designed to be light-weight, compact, highly efficient, and well suited for monolithic integration [1]-[3]. Depending on the switching pattern of the SC converter, most of the SC converters can be grouped into two major categories. Some of the SC converters can be controlled using a two-phase, non-overlapping clock [1][5]-[7], and other SC converters require more complex switching patterns [2][8]-[11]. In this paper, these two categories will be referred as two-phase and multi-phase SC converter respectively. The multi-phase SC converters are non-modular and require complex control compared to the two-phase SC converters. Among the two-phase SC converters, the multilevel modular capacitor clamped converter (MMCCC) topology is completely modular and possesses many advantageous features. MMCCC is bi-directional, scalable to any number of modules, can achieve high conversion ratio (CR) without increasing the voltage stress of the switches, can be used for multiple load-source integration and possesses a high utilization factor. The conversion ratio of an MMCCC is an integer in both step up and step down mode [5][12]-[19], and MMCCC can be programmed to achieve variable integer conversion ratios.

Although variable CRs can be achieved using MMCCC, it is limited to the integer numbers only. It has been proved that for a constant switching frequency, the realizable conversion ratio of an SC dc-to-dc voltage multiplier is fixed to a set of fractional numbers limited by the number of capacitor used [1][6][20]. In this paper two different methods have been proposed for MMCCC in order to achieve fractional variable CRs without altering the two-phase switching pattern. The first method is to switch the MMCCC at different frequencies such that the equivalent output resistance (EOR) acts as a voltage divider with the load. The constraint on the load resistance in order to achieve full dynamic range of CR has been analyzed in section III. The second method requires a different switching pattern which is generated by comparing a variable amplitude square wave with a lower frequency fixed amplitude triangular wave. Throughout the paper, these methods will be termed as variable frequency switching (VFS) and pulse dropping technique (PDT) respectively. For an ideal MMCCC with *k* active modules in step-up mode, the output voltage is (*k*+1) times the low side voltage. It has been observed that by lowering the operating switching frequency (VFS) or by varying the amplitude of the square wave (PDT), the CR can be varied in between (*k*+1) and *k*. Therefore, by using the proposed techniques in this paper and by changing the number of active modules, it is possible to achieve a wide range of continuously varying CR using MMCCC. However, the dynamic range of the output voltage variation depends on
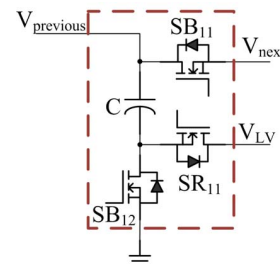

Fig. 1. Schematic of an MMCCC module.

the ratio of equivalent output resistance and the load resistance connected at the output of the MMCCC.

II. MMCCC TOPOLOGY

MMCCC is a modular two-phase SC converter where each module is constructed from one capacitor and three switching devices as shown in Fig. 1. For a k-module MMCCC, it requires $(3k+1)$ transistors, $(k+1)$ capacitors for a maximum conversion ratio of $(k+1)$. The maximum voltage stress on the switches is two times the low side input voltage regardless of the number of active modules. The schematic diagram of a 5-module MMCCC and the complementary switching patterns are shown in Fig. 2. Here, V_{LV} is the input voltage for step up mode. During the first segment of the clock cycle, the SR transistors are activated (ON), and the SB transistors are activated during the second phase of the clock. The detail operating principle of the MMCCC can be found in [5][12]-[19].

III. ESTIMATION OF EQUIVALENT OUTPUT RESISTANCE OF MMCCC

SC converters can be modeled as an ideal transformer and an equivalent series resistance at the output as outlined in [20]-[23], and the equivalent circuit is shown in Fig. 3, where R_{eqv} represents the equivalent output series resistance of the converter. A variable conversion ratio can be achieved by exploiting the equivalent output resistance of the MMCCC. A method of estimating equivalent output resistance (EOR) using state space modeling technique has been discussed in [23]. This equivalent resistance depends on the capacitance and equivalent series resistance (ESR) of the capacitors, ON-resistance of the switches, number of active modules and the switching frequency.

During each state of operation of a k-module MMCCC, KVL and KCL are applied in order to derive k independent equations relating the capacitor voltages and currents and written in the form shown in equation (1).

$$E_s i + F_s v + G_s u = 0 \qquad (1)$$

Here, suffix s indicates the state index; $s=1$ when SR switches are activated, and $s=2$ when SB switches are activated. Column vectors v and i contain all the capacitor voltages and currents respectively. Vector u consists of the input and output voltages of the converter: $u=[V_{in} \ V_{out}]^T$. Matrices E, F, G during two switching states of a 5-module
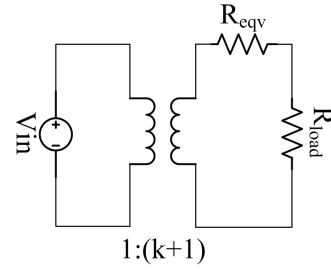

1:(k+1)

Fig. 2. Transformer model for SC converters in up-conversion mode.

$$E_1 = \begin{bmatrix} 2R_{sw} + R_C & 0 & 0 \\ 0 & 0 & 3R_{sw} + 2R_C \\ 0 & 1 & 1 \end{bmatrix}$$

$$F_1 = \begin{bmatrix} 1 & 0 & 0 \\ 0 & -1 & 1 \\ 0 & 0 & 0 \end{bmatrix}$$

$$G_1 = \begin{bmatrix} -1 & 0 \\ -1 & 0 \\ 0 & 0 \end{bmatrix}$$

$$E_2 = \begin{bmatrix} 0 & 3R_{sw} + 2R_C & 0 \\ 0 & 0 & -(2R_{sw} + R_C) \\ 1 & 1 & 0 \end{bmatrix}$$

$$F_2 = \begin{bmatrix} -1 & 1 & 0 \\ 0 & 0 & -1 \\ 0 & 0 & 0 \end{bmatrix}$$

$$G_1 = \begin{bmatrix} -1 & 0 \\ -1 & 1 \\ 0 & 0 \end{bmatrix}$$

(2)

MMCCC are given in equation (2). Here, the vectors E, F, G contain the coefficients of the KVL and KCL equations obtained during both states of MMCCC.

Here, R_{sw} and R_C are the ON-resistance of each switches and ESR of each of the capacitors respectively. In [20]-[21], a simpler method of calculating EOR has been introduced in terms of slow switching limit (SSL) and fast switching limit (FSL). As the MMCCC circuit is being operated at considerably low frequency, the fast switching limit can be ignored here. Using the methods outlined in [20]-[21], the slow switching limit for k-module MMCCC can be written as
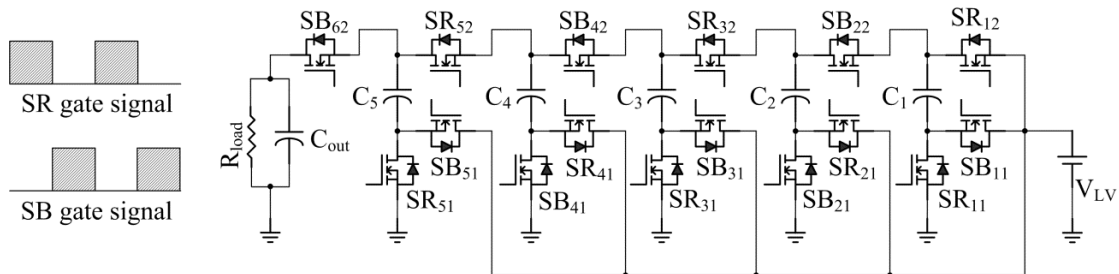

Fig. 2. A 5-module MMCCC and complementary gate signals.

shown in equation (3).

$$R_{SSL} = \frac{k}{C f_{sw}} \qquad (3)$$

Here, C is the capacitance used in each module and f_{sw} is the switching frequency. The EOR of MMCCC for different number of active modules using both the above mentioned methods is shown in Fig. 4 and the calculated EOR using both methods highly conforms to each other. The physical parameters such as capacitance, ESR of the capacitor and the ON-resistance of the MOSFETs are collected from the datasheets of the components used. Based on these parameters, EOR of MMCCC increases exponentially as the switching frequency decreases. Similarly, the EOR of the MMCCC at constant frequency increases with the increased number of active modules. For a k-module MMCCC, the minimum EOR required (R_{EOR_req}) for a dynamic range of CR variation equal to 1 is given in equation (4).

$$R_{EOR\_req} = \frac{R_{load}}{k} \qquad (4)$$

Here, R_{load} is the load resistance connected at the output of the MMCCC, and k is the number of active modules. The efficiency of the converter decreases with the increase in EOR and according to equation (4), it is possible to lower the CR with relatively smaller drop in efficiency if additional modules are activated.

IV. SWITCHING SCHEMES

Using variable frequency switching (VFS), variable CR can be achieved by varying the operating frequency of the MMCCC, and the required minimum operating frequency can be found using equation (3)-(4). MMCCC is required to operate at a switching frequency so that EOR is smaller than R_{EOR_req}. Similar variation in CR can be achieved by varying the amplitude of the square wave using pulse dropping technique (PDT). Similar to SPWM, two modulation indexes can be introduced for PDT: amplitude modulation index (m_a) and frequency modulation index (m_f). Amplitude modulation index can be defined as in equation (5).

$$m_a = \frac{\widehat{v}_{sqr}}{\widehat{v}_{tri}} \qquad (5)$$

Where, $\widehat{v}_{sqr}$ is the amplitude of the square wave signal and $\widehat{v}_{tri}$ is the amplitude of the triangular wave and m_a can be varied from 0 to 1.

Similarly, the frequency modulation index may be defined as in equation (6).

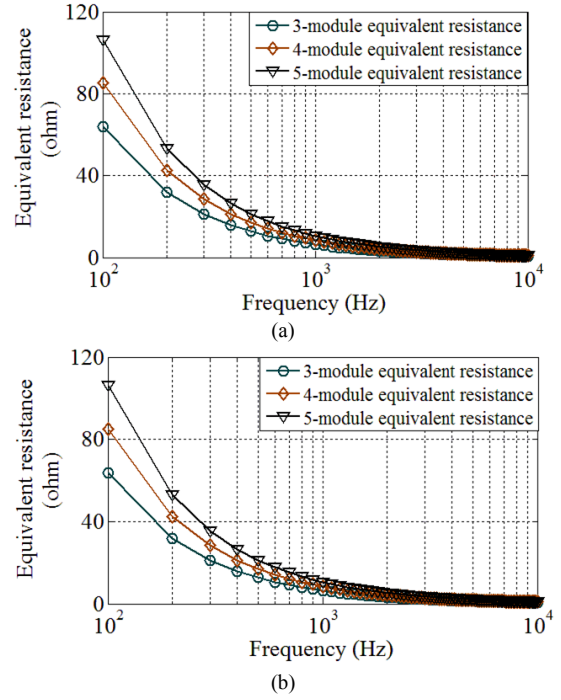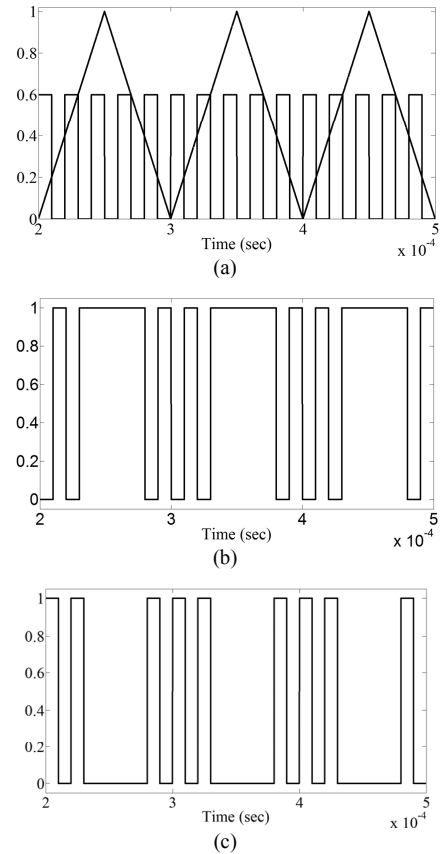$$m_f = \frac{f_{sqr}}{f_{tri}} \qquad (6)$$

Fig. 4. Equivalent output resistance of MMCCC for different number of active modules are shown in (a) using state space model and in (b) using slow switching limit.
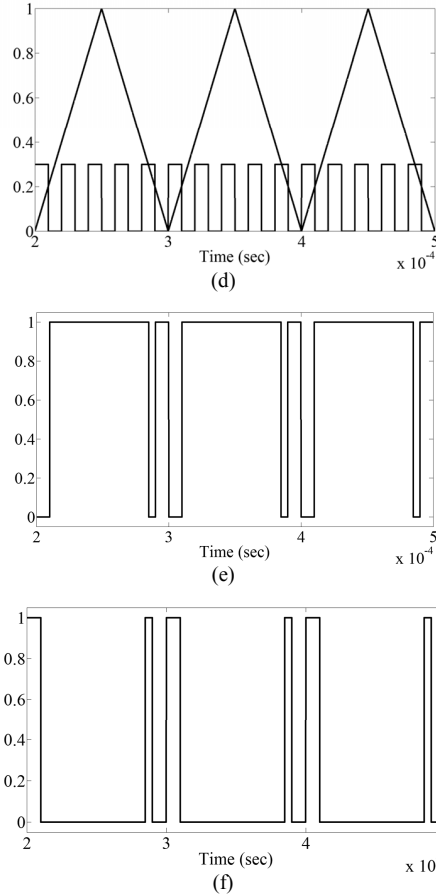
(d)

(e)

(f)

Fig. 5. For (a)-(c), m_a=0.6 and for (d)-(f), m_a=0.3. Square wave of different amplitudes with fixed amplitude triangular wave are shown in (a) and (d). Complementary gate signals for m_a=0.6 are shown in (b)-(c). Complementary gate signals for m_a=0.3 are shown in (e)-(f).

Here, f_{sqr} and f_{tri} are the frequencies of the square wave signal and the triangular waveform respectively. In Fig. 5, the detail of the construction of the gate signals are shown with m_a=0.6 and 0.3, and m_f = 5.

It should be noted that the resulting clock signals consist of two different segments depending on the values of m_a and m_f. One segment consists of pulses with fixed pulse width equal to $1/f_{sqr}$. Pulses having smaller width might occur at the boundaries of this section as shown in Fig. 5(e) and Fig. 5(f). Therefore, the MMCCC is switched at a constant frequency equal to f_{sqr} in this segment except at the boundaries. During the other segment, the gate signal is either 1 (Fig. 5(b) and Fig. 5(e)) or 0 (Fig. 5(c) and Fig. 5(f)) for longer time span depending on the values of m_a.

V. SIMULATION RESULTS

In order to verify the proposed control schemes, MMCCC consists of different number of modules were simulated in PSIM. All capacitors were simulated using fixed 470μf capacitor with 0.02 Ω equivalent series resistance (ESR). The ON resistance of all the MOSFETs was set to 0.01 Ω, and the
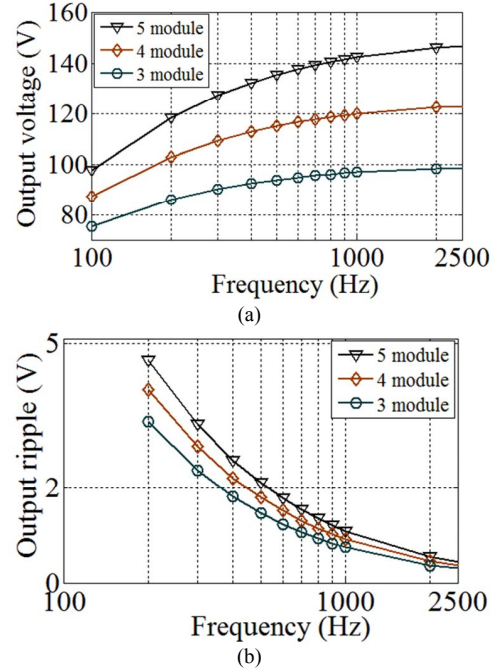

(a)

(b)

Fig. 6. Simulation results for (a) output voltage and (b) output ripple vs. frequency using VFS.
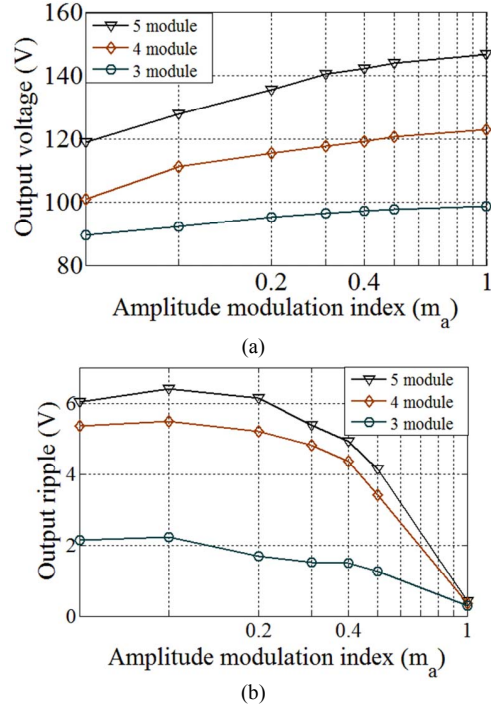

(a)

(b)

Fig. 7. Simulation results for (a) output voltage and (b) output ripple vs. amplitude modulation index (m_a) using PDT.

converter was loaded with a fixed 200 Ω resistive load. The switching frequency was varied from 100 Hz to 2500 Hz, and the variation in the output voltage (dc) and the output voltage ripple are shown in Fig. 6. As expected, the ripple component

increases with the increase in number of active modules and decreases with increased operating frequency.

Using PDT, the frequency of the square wave was fixed at 2500 Hz and the output voltage and amount of ripple were observed for different values of amplitude modulation index (m_a). The switching frequency of the triangular wave was set to 100 Hz, 200 Hz and 300 Hz for 5-module, 4-module and 3-module MMCCC respectively in order to get the required variation in CR using the same range of m_a. These variations in output voltage and output voltage ripple as a function of m_a are shown in Fig. 7. Similar to VFS, The output voltage ripple increases with increased in number of active modules and decreases with increased m_a.

VI.   EXPERIMENTAL RESULTS

A 5-module MMCCC prototype was built and tested in the laboratory setup in order to support the simulation results. The prototype was built in such a way that it can also be reconfigured into a 3- or 4-module MMCCC by bypassing one or two modules. The maximum voltage stress of the upper MOSFET of each module (SB_{11} in Fig. 1) is two times the input voltage, and these switches have been implemented using 150 V 34 A N-channel switches IRFI4228PBF. The maximum voltage stress of other two MOSFETs of each module (SR_{11} and SB_{12} in Fig. 1) is equal to the amplitude of the low voltage side input voltage and implemented using 100 V 43 A N-channel switches IRFI4410ZPBF, and an 470 μF electrolytic capacitor was used in each module of the
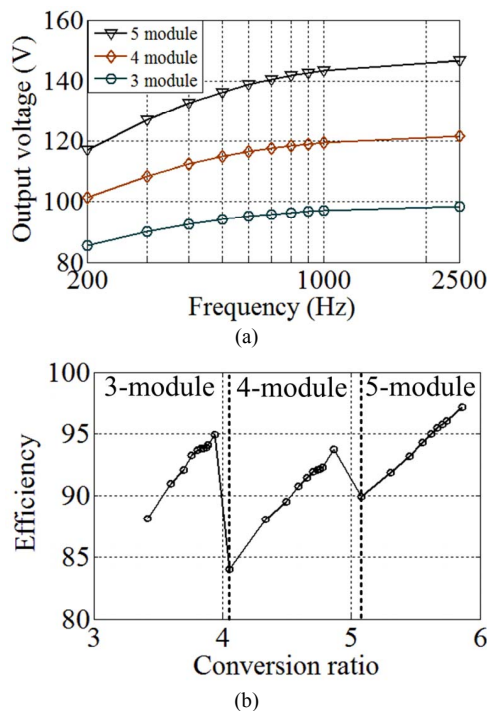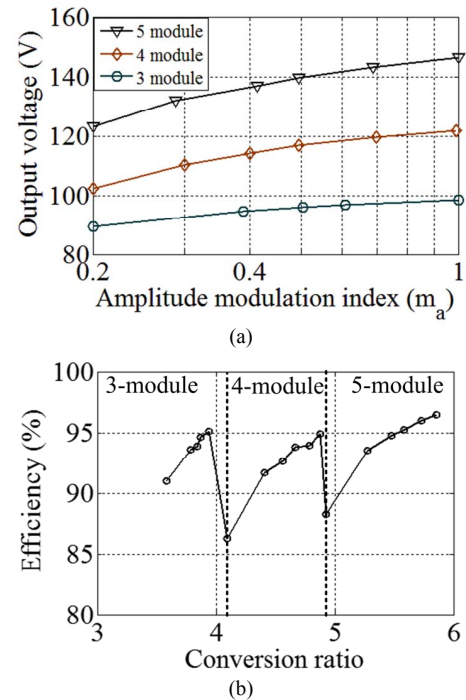

(a)

(b)

Fig. 9. Experimental results for (a) output voltage and (b) efficiency vs. amplitude modulation index (m_a) using PDT.

Fig. 10. Reconfigurable 5-module MMCCC prototype

circuit. A 3711A DC electronic load was used as a resistive load. The resistance of the electronic load was set at 200 Ω. The input and output power were measured using Digital power analyzer 3430-3HS from valhalla Scientific Inc. and PM3000ACE-001 three phase power analyzer from Voltech Instruments Ltd., respectively. The experimental results showing CR variation and efficiency at different CR for 3- to 5-module MMCCC for VFS and PDT are shown in Fig. 8 and Fig. 9 respectively, and the prototype is shown in Fig. 10. In Fig. 8(a), the output voltage is plotted against the switching frequency and in Fig. 9(a), the output voltage is plotted against amplitude modulation index (m_a). Similar variation in the output voltage is observed using both techniques. In Fig. 8(b) and Fig. 9(b), the efficiencies of the converter have been

(a)

(b)

Fig. 8. Experimental results for (a) output voltage and (b) efficiency vs. frequency using VFS.
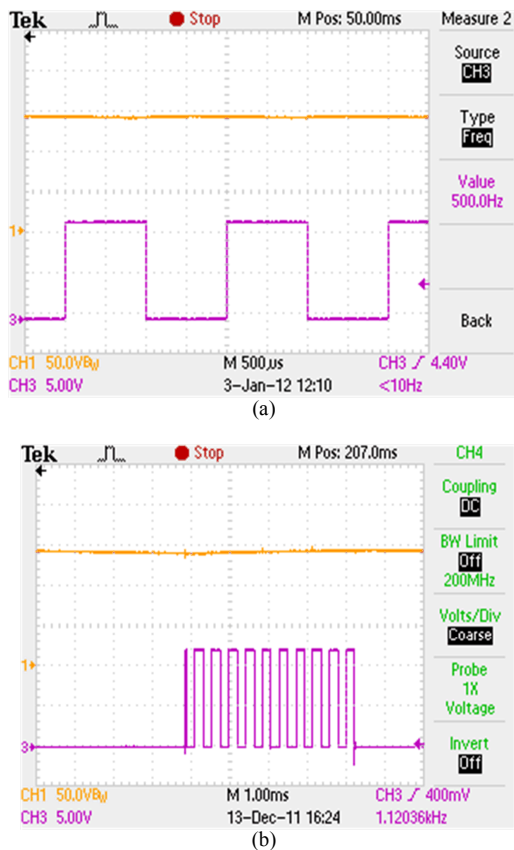
(a)

(b)

Fig. 11. Oscilloscope capture of the output voltage (Ch1- 50V/div) and gate signal (Ch3) for VFS and PDT are shown in (a) and (b), respectively. For VFS, the switching frequency is 500 Hz and for PDT, m_a was set to 0.45.

plotted against various CRs. Two oscilloscope captures of gate signals and output voltages using VFS and PDT are shown in Fig. 11. The average of the conversion efficiency was around 90% to achieve continuously variable conversion ratio.

VII. CONCLUSIONS

Two different techniques for achieving fractional and continuously variable conversion ratio using MMCCC have been discussed. The variation of conversion ratio by changing the operating frequency is well known for switched capacitor converters, and the second method of varying conversion ratio proposed in this paper provides additional degree of freedom for achieving wide range of output voltage regulation using MMCCC. The equivalent output resistance variation as a function of the operating frequency of the MMCCC has been analyzed using two different well known techniques. The variation of output voltage ripple and efficiency vs. conversion ratio are also analyzed. Finally, the concepts are validated using both simulations and experiments using a reconfigurable 5-module MMCCC prototype circuit.

REFERENCES

[1] M. S. Makowski and D. Maksimovic, "Performance limits of switched-capacitor dc-dc converters," IEEE Power Electronics Specialists Conference, vol. 2, pp. 1215-1221, June 1995.

[2] Z. Pan, F. Zhang, and F. Z. Peng, "Power losses and efficiency analysis of multilevel dc-dc converters," IEEE Applied Power Electronics Conference, pp. 1393-1398, March 2005.

[3] Michael D. Seeman ,"A Design Methodology for Switched-Capacitor DC-DC Converters," Ph.D. Dissertation, University of California at Berkeley, May 2009, available at: URL: http://www.eecs.berkeley.edu/Pubs/TechRpts/2009/EECS-2009-78.pdf

[4] M.D. Seeman, V.W. Ng, Hanh-Phuc Le, M. John, E. Alon, S. R. Sanders, "A comparative analysis of Switched-Capacitor and inductor-based DC-DC conversion technologies", COMPEL 2010, pp. 1-7.

[5] F. H. Khan, L. M. Tolbert, "A Multilevel Modular Capacitor Clamped DC_DC Converter," IEEE Industry Applications Society (IAS) Conference, Tampa, FL, Oct. 2006, pp. 966-973 (Award paper).

[6] M. S. Makowski, "Realizability conditions and bounds on synthesis of switched-capacitor DC-DC voltage multiplier circuits," IEEE Trans. Circuits and System-I, pp.684-691, Aug 1997.

[7] O. Wong, W. Tam, C. Kok, H. Wong, "Design strategy for 2-phase switched capacitor charge pump", IEEE APCCAS 2008, pp. 1328 – 1331.

[8] F. Z. Peng, F. Zhang, and Z. Qian, "A novel compact DC–DC converter for 42 V systems," in *Proc. IEEE Power Electron. Spec. Conf.*, Jun. 2003, pp. 33–38.

[9] On-Cheong Mak, Yue-Chung Wong, and Adrian Ioinovici, "Step-up DC Power Supply Based on a Switched-Capacitor Circuit," IEEE Trans. of Industrial Electronics,vol. 42, no. 1, Feb. 1995, pp. 90-97.

[10] S. V. Cheong and H. Chung, "Inductorless DC-to-DC Converter with High Power Density," IEEE Trans. of Industrial Electronics, vol. 41, no. 2, Apr. 1994, pp. 208-215

[11] Tohru Umeno, Kiyoshi Takahashi, Ichirou Oota, Fumio Ueno, and Takahiro Inoue, "New Switched-Capacitor DC-DC Converter With Low Input Current and Its Hybridization," Proceedings of the 33rd Midwest Symposium on Circuits and Systems, Aug. 1990, vol. 2, pp. 1091-1094

[12] F. H. Khan, L. M. Tolbert, "A Multilevel Modular Capacitor Clamped DC_DC Converter," IEEE Industry Applications Society (IAS) Conference, Tampa, FL, Oct. 2006, pp. 966-973 (Award paper).

[13] F. H. Khan, L. M. Tolbert, "Multiple Load-Source Integration in a Multilevel Modular Capacitor Clamped DC-DC Converter Featuring Fault Tolerant Capability," IEEE Applied Power Electronics Conference (APEC), Anaheim, CA, Feb. 2007, pp. 361-367.

[14] F. H. Khan, L. M. Tolbert, "Universal Multilevel DC-DC Converter with Variable Conversion Ratio, High Compactness Factor and Limited Isolation Feature," IEEE Applied Power Electronics Conference (APEC), Austin, TX, February 2008, pp. 17-23.

[15] F. H. Khan, L. M. Tolbert, "Generating Isolated Outputs in a Multilevel Modular Capacitor Clamped DC-DC Converter (MMCCC) for Hybrid Electric and Fuel Cell Vehicles," IEEE Power Electronics Specialists Conference (PESC), Rhodes, Greece, June 2008, pp. 967-973.

[16] F. H. Khan, L. M. Tolbert, "A Multilevel Modular Capacitor-Clamped DC-DC converter," IEEE Transactions on Industry Applications, vol. 43, no. 6, pp. 1628-1638, Nov. 2007.

[17] F. H. Khan, L. M. Tolbert, "Bi-directional Power Management and Fault Tolerant Feature in a 5 kW Multilevel DC-DC Converter with Modular Architecture," IET Power Electronics, vol. 2, no. 5, pp. 595-604, Sept. 2009.

[18] F. H. Khan, L. M. Tolbert, "Multiple Load-Source Integration in a Multilevel Modular Capacitor Clamped DC-DC Converter Featuring Fault Tolerant Capability," IEEE Transactions on Power Electronics, vol. 24, no. 1, pp. 14-24, Jan. 2009.

[19] F. H. Khan, L. M. Tolbert, "Startup and Dynamic Modeling of the MMCCC Converter," IEEE Transactons on Power Electronics, vol. 25, no. 2, pp. 519-531, Feb. 2010. M. S. Makowski "Voltage regulation in switched-capacitor converters—A problem revisited", Proc. 5th Eur. Space Power Conf., p.357 , 1998

[20] M. D. Seeman and S. R. Sanders, "Analysis and optimization of switched capacitor DC-DC converters," in *Proc. IEEE Comput. Power Electron. Workshop*, 2006, pp. 216–224.

[21] M. D. Seeman and S. R. Sanders, "Analysis and optimization of switched capacitor dc-dc converters," IEEE Trans. Power Electron., vol. 23, no. 2, pp. 841–851, Mar. 2008.

[22] J. W. Kimball, P. T. Krein, and K. R. Cahill, "Modeling of capacitor impedance in switching converters," *IEEE Power Electron. Lett.*, vol. 3, no. 4, pp. 136–140, Dec. 2005.

[23] J. M. Henry, J. W. Kimball, "Practical Performance Analysis of Complex Switched-Capacitor Converters", IEEE Transactions on Power Electronics, vol. 26, issue. 1, pp. 127-136, Jan. 2011.